Available online at www.sciencedirect.com
SCIENCE DIRECT®
Physica A 356 (2005) 48–53
PHYSICA A
www.elsevier.com/locate/physa

Localized patterns and hole solutions in one-dimensional extended systems

Marcel G. Clerc*, Claudio Falcon

Departamento de Física, Facultad de Ciencias Físicas y Matemáticas, Universidad de Chile, Casilla 487-3, Santiago, Chile

Available online 13 June 2005

Abstract

The existence, stability properties, dynamical evolution and bifurcation diagram of localized patterns and hole solutions in one-dimensional extended systems are studied from the point of view of front interactions. An adequate envelope equation is derived from a prototype model that exhibits these particle-like solutions. This equation allows us to obtain an analytical expression for the front interaction, which is in good agreement with numerical simulations.

PACS: 47.54.+r; 45.70.Qj

Keywords: Fronts; Patterns; Localized structures

Non-equilibrium processes often lead by nature to the formation of spatial periodic structures developed from a homogeneous state through the spontaneous breaking of symmetries present in the system [1,2]. In the last decade localized patterns or localized structures have been observed in different experiments: liquid crystals [3], gas discharge systems [4], chemical reactions [5], fluids [6], granular media [7], and nonlinear optics [8,9]. One can understand these localized patterns as patterns extended only over a small portion of an extended system. From the point of view of dynamics, the localized patterns in one-dimensional spatial systems are

*Corresponding author.
E-mail address: marcel@dfi.uchile.cl (M.G. Clerc).

0378-4371/$ - see front matter © 2005 Published by Elsevier B.V.
doi:10.1016/j.physa.2005.05.011

homoclinic connections for the stationary dynamical system [10]. Recently, a geometrical interpretation of the existence, stability properties, and bifurcation diagram of localized patterns in one-dimensional extended systems has been given [11].

The aim of this paper is to describe how one-dimensional localized patterns and hole solutions arise from front interactions. From a prototype model that exhibits localized patterns and hole solutions, the subcritical Swift–Hohenberg equation, we deduce an adequate equation for the envelope of these particle-like solutions. This model has a front solution that connects a stable homogeneous state with a stable spatially periodic one. Due to the oscillatory nature of the front interaction, which alternates between attractive and repulsive, we can infer the existence, stability properties, dynamical evolution and bifurcation diagram of localized patterns and hole solutions. Hence, we reobtain the bifurcation diagram of localized patterns and hole solution deduced from the horseshoe behavior of the attractive and repulsive manifold of ordinary differential equations [11].

Let us consider a prototype model that exhibits localized patterns and hole solutions in a one-dimensional extended system, the subcritical Swift–Hohenberg equation [12] is

$$\partial_t u = \varepsilon u + v u^3 - u^5 - (\partial_{xx} + q^2)^2 u \,, \tag{1}$$

where $u(x,t)$ is an order parameter, $\varepsilon - q^4$ is the bifurcation parameter, q is the wavenumber of periodic spatial solutions, and v is the control parameter of the type of bifurcation, supercritical or subcritical. This model describes the confluence of a stationary and a spatial subcritical bifurcation, when the parameters scale as $u \sim \varepsilon^{1/4}$, $v \sim \varepsilon^{1/2}$, $q \sim \varepsilon^{1/4}$, $\partial_t \sim \varepsilon$ and $\partial_x \sim \varepsilon^{1/4}$ ($\varepsilon \ll 1$). It is often employed in the description of patterns observed in Rayleigh–Benard convection and pattern-forming systems [2]. In Fig. 1 we show typical localized patterns, hole solutions, and motionless front solutions obtained from this model. For small and negative v, and $9v^2/40 < \varepsilon < 0$, the system exhibits coexistence between a stable homogeneous state $u(x) = 0$ and a periodic spatial one $u(x) = \sqrt{v}(\sqrt{2(1+\sqrt{1+40\varepsilon/9v^2})}\cos(qx)) + o(v^{5/2})$. In this parameter region, one finds a front between these two stable states (cf. Fig. 1). In order to describe the front, localized patterns and hole solutions, we introduce the ansatz

$$u = \sqrt{\frac{2v}{10}}\varepsilon^{1/4}\left\{A\left(y = \frac{3\sqrt{|\varepsilon|}}{2\sqrt{10q}}x,\ \tau = \frac{9v^2|\varepsilon|}{10}t\right) + w_1(x,y,\tau)\right\}e^{iqx} + c.c \,, \tag{2}$$

where $A(y,\tau)$ is the envelope of the front solution, $w_1(x,y,\tau)$ is a small correction function of order ε, and $\{y,\tau\}$ are slow variables. Note that in this ansatz we consider that q is order one, or larger than the other parameters. Introducing the above ansatz in Eq. (1) and linearizing in w_1, we find the following solvability condition:

$$\partial_\tau A = \varepsilon A + |A|^2 A - |A|^4 A + \partial_{yy} A + \left(\frac{A^3}{9v} - \frac{A^3|A|^2}{2}\right)e^{a\frac{2iqy}{\sqrt{|\varepsilon|}}} - \frac{A^5}{10}e^{a\frac{4iqy}{\sqrt{|\varepsilon|}}} \,, \tag{3}$$

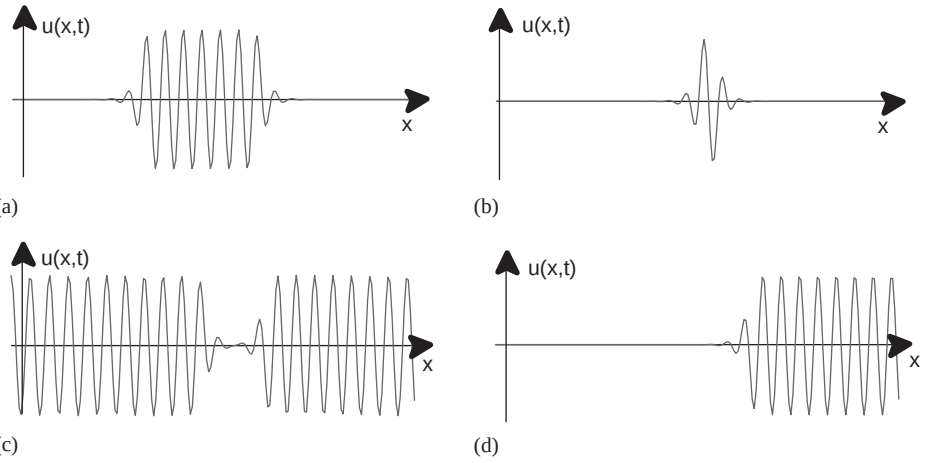

Fig. 1. Particle-type solutions appearing in the subcritical Swift–Hohenberg equation. The parameters have been chosen as $\varepsilon = -0.16$, $v = 1.00$, and $q = 0.70$. (a) Localized pattern, (b) shortest localized pattern, (c) hole solution and (d) front solution.

where $\varepsilon \equiv 10\varepsilon/9v^2$, and $a \equiv 3v/2\sqrt{10}q$. The terms proportional to the exponential are non-resonant, that is, one can eliminate these terms by an asymptotic change of variables. Furthermore, they have rapidly varying oscillations in the limit $\varepsilon \to 0$. Hence, one usually neglects these terms. Note that the above envelope equation is a universal model, close to a spatial bifurcation, of a system that exhibits coexistence between a homogeneous state and a spatially periodic one. In general, one can use an ansatz similar to (2) and noting that the envelope satisfies independently the symmetries $\{x \to -x, A \to \bar{A}\}$ and $\{x \to x + x_o, A \to A\mathrm{e}^{\mathrm{i}qx_o}\}$ one derives Eq. (3).

When one considers only the resonant terms, that is, when all spatial-forcing terms are neglected, it is straightforward to show that the system has a front solution between two homogeneous states, 0 and $\sqrt{(1+\sqrt{1+4\varepsilon})/2}$, when $-1/4 < \varepsilon < 0$. This front propagates from the global stable (global minimum) to a metastable one (local minimum). At the Maxwell point, where the equilibrium states have the same energy, the front is motionless. This point is reached at $\varepsilon_M = -3/16$, where the front solution has the form

$$a_{\pm}(y) = \sqrt{\frac{3/4}{1+\mathrm{e}^{\pm\sqrt{3/4}(y-y_o)}}}\,\mathrm{e}^{\mathrm{i}\theta},$$

where y_o is the front's core position, and θ is an arbitrary phase.

To describe a localized pattern exhibited by (1) as the interaction of two fronts, we must then consider the non-resonant terms in the envelope equation (3). We consider all these terms as perturbations because they have rapidly varying oscillations. Close

to the Maxwell point, we use the ansatz

$$A_{LP}(y,\tau) = \left[a_-(y - y_1(\tau)) + a_+(y - y_2(\tau)) - \sqrt{\frac{3}{4}} + \rho(y_1, y_2, y, \tau)\right] e^{i\theta(y_1,y_2,y,\tau)},$$

where $\{\rho, \theta\}$ are small correction functions, which are of order $\delta\varepsilon \equiv (\varepsilon - \varepsilon_M)$ and $y_2 > y_1$. Introducing the above ansatz in Eq. (3), linearizing in $\{\rho, \theta\}$ and after straightforward calculations, we obtain the following solvability condition for the distance between the fronts:

$$\frac{d\Delta}{d\tau} = f(\Delta) \equiv -\alpha\Delta \exp\left(-\sqrt{\frac{3}{4}}\Delta\right) + \beta\cos(2q\Delta/\sqrt{\varepsilon}) + 2\delta\varepsilon\,, \tag{4}$$

where $\Delta \equiv y_2 - y_1$, $\alpha = 27\sqrt{3}/64$ and $\beta = 64\sqrt{3}q^2\exp(-q4\pi/\sqrt{\varepsilon})/3\varepsilon$. In Fig. 2, we display the interaction between two fronts. It is important to notice that in one-dimensional extended systems, the dependence of the front interaction on the front distance (Δ) is purely exponential [2]. In the present case, the linear and periodic dependence on Δ is a consequence of the interaction (contained in the non-resonant terms) of the large scale with the small scale of the underlying spatially periodic solution. The system has several equilibria, $f(\Delta^*) = 0$, that are stable if $f'(\Delta^*) < 0$. Thus, the existence and stability of localized patterns are given by the oscillatory nature of the front interaction. As is illustrated in Fig. 2, each region of attractive and repulsive interaction is separated by localized patterns. It is also important to notice that the larger equilibrium (Δ^*) represents localized patterns with a larger number of bumps.

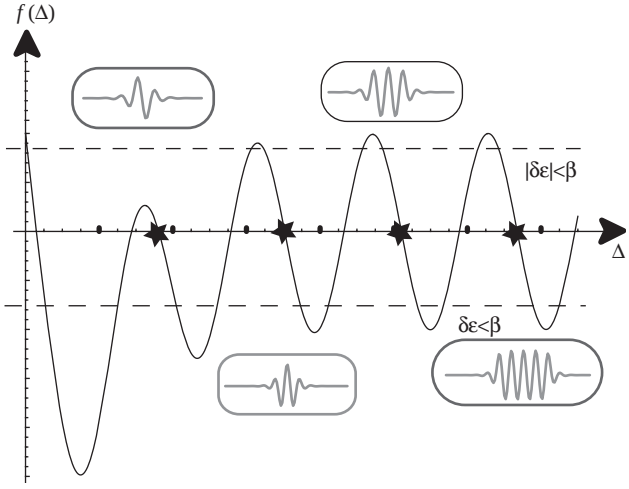

Fig. 2. Oscillatory interaction force $f(\Delta)$. The inset figures show the stable localized patterns observed at the Maxwell point. The lengths of these localized patterns are represented by the stars. The dashed lines represent the effective abscissas that determine the size of localized patterns when ε is changed.

In order to understand the bifurcation diagram of localized patterns, we consider the effect of changing the bifurcation parameter ε. Modifying ε is equivalent to moving the abscissa on the graph of front interaction (cf. Fig. 2). First, we consider the case $|\delta\varepsilon| > \beta$ and $\delta\varepsilon < 0$; the interaction is always attractive, that is, there is no equilibrium. Hence, if one takes into account a front that connects the homogeneous state with the spatially periodic state, then the spatially periodic state invades the homogeneous one. On increasing ε, one finds the first equilibrium point $\Delta = \infty$ for $\delta\varepsilon = \delta\varepsilon_- \equiv \beta$ and $\delta\varepsilon < 0$. Here, the system has a motionless front between the spatially periodic state and the homogeneous one. This front remains stationary until $|\delta\varepsilon| \leqslant \beta$; therefore, this front is motionless in a parameter range. This phenomenon is well-known as the *Locking phenomenon* and the interval $|\delta\varepsilon| \leqslant \beta$ is the denominated pinning range [13]. For $\delta\varepsilon > \beta$, the front propagates from the spatially periodic state to the homogeneous one. In Fig. 3, the thick solid line shows the velocity of front propagation as a function of the bifurcation parameter.

Increasing $\delta\varepsilon$ from $\delta\varepsilon_-$, we observe that the equilibria, that is, localized patterns, appear by successive saddle-node bifurcations each time with a length smaller than the previous one, i.e., the localized patterns appear by pairs, one stable and another unstable, and each time with a smaller number of bumps. This sequence of bifurcations is illustrated in Fig. 3 by the points c_i^a. For small, $\delta\varepsilon$ and close to the Maxwell point, the system has an infinite number of localized patterns with all the possible number of bumps. The lengths of the localized patterns are roughly multiples of that of the shortest localized state (one bump). In contrast, for $|\delta\varepsilon| > \beta$, the localized patterns disappear by saddle-node bifurcations and with increasing $\delta\varepsilon$ the larger localized patterns disappear one after the other. Hence, the shortest localized state is the last to disappear. In Fig. 3 the sequences of these bifurcation are represented by the points c_i^d.

Model (1) has different particle-like solution fronts, localized patterns and holes. These solutions are displayed in Fig. 1. From the front interaction the hole solutions

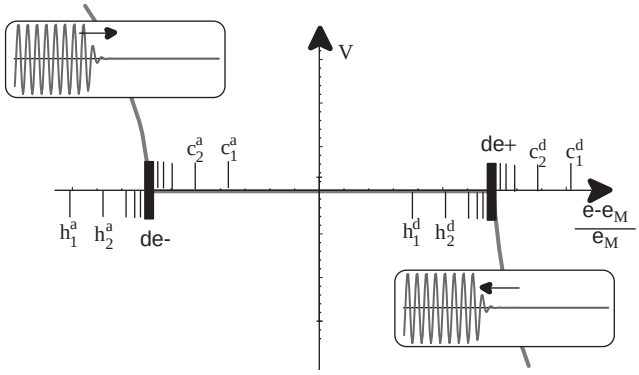

Fig. 3. Speed of the front and bifurcation diagram of the localized patterns and hole solutions as a function of the bifurcation parameter. The thick solid line indicates the front velocity. c_i^a and c_i^d (h_i^a and h_i^d) represent the bifurcation points where the localized patterns with (hole solutions without) i-bumps appear and disappear, respectively.

can be understood as the *complementary of localized patterns*, because these solutions can be described in terms of the front as

$$A_{hole}(y,\tau) = (a_+(y - y_2(\tau)) + a_-(y - y_2(\tau)) - \rho(y_1, y_2, y, \tau))e^{i\theta(y_1,y_2,y,\tau)},$$

where this solution asymptotically converges to a spatially periodic state. We obtain the same expression for interaction (4) by replacing α by $-\alpha$. Therefore, for these solutions, on increasing ε we obtain a bifurcation diagram similar to that of localized patterns but inverted, that is, the first hole appearing and disappearing by saddle-node bifurcation is the shortest one. Successively, the holes with larger length appear one after the other. Then, the solutions with shorter length disappear sequentially one after the other. In Fig. 3 this sequence of bifurcations is indicated by the points $\{h_i^a, h_i^d\}$.

It is important to remark that the bifurcation diagram shown in Fig. 3 has been deduced from geometrical arguments based on the horseshoe behavior of the attractive and repulsive manifolds of an ordinary differential equation [11]. Adding to the previous results, the front interaction also allows us to predict the dynamical evolution of localized structures. In the pinning range, the front solution is motionless. Recently, it has been shown that additive white noise induces front propagation close to the pinning range [14]. The mean velocity of the front is zero only in the Maxwell point, that is, at the Maxwell point the front core describes a Brownian motion.

In conclusion, we have shown on the basis of the front interactions the existence, stability properties, dynamical evolution and bifurcation diagram of localized patterns and hole solutions in one-dimensional extended systems.

The authors would like to thank S. Residori, R. Rojas, and E. Tirapegui for fruitful discussions. The simulation software *DimX* developed by P. Coullet and collaborators at the laboratory INLN in France has been used for all the numerical simulations. The authors acknowledge the support of FONDECYT project 1051117, FONDAP grant 11980002, and the ECOS-CONICYT collaboration program.

References

[1] G. Nicolis, I. Prigogine, Self-organization in Non Equilibrium Systems, Wiley, New York, 1977.
[2] M. Cross, P. Hohenberg, Rev. Mod. Phys. 65 (1993) 851.
[3] S. Pirkl, P. Ribiere, P. Oswald, Liq. Cryst. 13 (1993) 413.
[4] Y.A. Astrov, Y.A. Logvin, Phys. Rev. Lett. 79 (1997) 2983.
[5] K.J. Lee, W.D. McCormick, Q. Ouyang, H. Swinney, Science 261 (1993) 192.
[6] O. Lioubashevski, Y. Hamiel, A. Agnon, Z. Reches, J. Fineberg, Phys. Rev. Lett. 83 (1999) 3190.
[7] P.B. Umbanhowar, F. Melo, H. Swinney, Nature 382 (1996) 793.
[8] F.T. Arecchi, S. Boccaletti, P.L. Ramazza, Phys. Rep. 318 (1999) 1.
[9] B. Schapers, M. Feldmann, T. Ackemann, W. Lange, Phys. Rev. Lett. 85 (2000) 748.
[10] W. van Saarloss, P.C. Hohenberg, Phys. Rev. Lett. 64 (1990) 749.
[11] P. Coullet, C. Riera, C. Tresser, Rev. Lett. 84 (2000) 3069.
[12] H. Sakaguchi, H. Brand, Physica D 97 (1996) 274.
[13] Y. Pomeau, Physica D 23 (1986) 3.
[14] M.G. Clerc, C. Falcon, E. Tirapegui, Phys. Rev. Lett. submitted for publication.